Q-branch linewidths of N2 perturbed by H2: experiments and quantum calculations from an ab initio potential.

Laura Gómez, Raúl Z Martínez, Dionisio Bermejo, Franck Thibault, Pierre Joubert, Béatrice Bussery-Honvault, Jeanine Bonamy

Q -branch linewidths of N 2 perturbed by H 2 : Experiments and quantum calculations from an ab initio potential

Laura Gómez, Raúl Z. Martínez, Dionisio Bermejo, Franck Thibault, Pierre Joubert, Béatrice Bussery-Honvault, and Jeanine Bonamy

Citation: The Journal of Chemical Physics **126**, 204302 (2007); doi: 10.1063/1.2731789
View online: http://dx.doi.org/10.1063/1.2731789
View Table of Contents: http://scitation.aip.org/content/aip/journal/jcp/126/20?ver=pdfcov
Published by the AIP Publishing

Q-branch linewidths of N_2 perturbed by H_2: Experiments and quantum calculations from an *ab initio* potential

Laura Gómez, Raúl Z. Martínez, and Dionisio Bermejo
Instituto de Estructura de la Materia, CSIC, Serrano 123, 28006 Madrid, Spain

Franck Thibault
Laboratoire PALMS, UMR CNRS 6627, Université de Rennes I, 35042 Rennes Cedex, France

Pierre Joubert,[a] Béatrice Bussery-Honvault, and Jeanine Bonamy
Institut UTINAM, UMR CNRS 6213, Université de Franche-Comté, 25030 Besançon Cedex, France

(Received 22 February 2007; accepted 26 March 2007; published online 22 May 2007)

In this work the authors present an experimental and theoretical study about the *Q*-branch lines' broadening coefficients of N_2 perturbed by H_2. Experimental values for these parameters have been obtained at 440 and 580 K, and quantum calculations have been performed using a new *ab initio* potential energy surface, obtained by quantum chemistry methods. The results of these calculations are compared to experimental data obtained previously at 77 and 298 K [L. Gomez *et al.*, Mol. Phys. **104**, 1869 (2006)] and to the present measurements. A satisfactory agreement is obtained for the whole range of temperatures used in the experiments. © *2007 American Institute of Physics*. [DOI: 10.1063/1.2731789]

I. INTRODUCTION

In the last decades, laser spectroscopic techniques have been greatly improved, in particular, their applications to atmospheric monitoring and combustion diagnostics. But, a reliable interpretation of the quantitative measurements requires an accurate knowledge of the collisional parameters such as the line shifting and line broadening coefficients of the molecular species constituting these media.

The nitrogen molecule is one of the major active molecules used for thermometry in combustion media. This is why N_2 has often been used as a probe molecule for the determination of local temperature or concentration. Numerous studies concerning pure N_2 systems have been carried out[1,2] using Raman spectroscopy. Precise studies of the collisional processes involving N_2 as an active molecule are also essential in atmospheric applications at lower temperatures. However, apart from pure N_2 (Refs. 1 and 2) or N_2-H_2O (Ref. 3) systems, few data are available in the literature involving N_2 as active molecule.

In a previous work,[4] we have presented for the first time the experimental and theoretical values for the collisional line broadening coefficients of the N_2-H_2 system. The measurements were obtained from high resolution stimulated Raman spectra recorded in Madrid at 77 and 298 K. Theoretical calculations between 77 and 500 K were performed using the semiclassical Robert-Bonamy (RB) model.[5] At room temperature, both experimental and theoretical values showed a good agreement using an adjusted value for the kinetic diameter of the atom-atom potential used in the RB model. However, we observed a discrepancy at 77 K attributed to orbiting collisions, which are not taken into account in the semiclassical model.

In this work, we present new measurements of N_2 *Q*-branch lines broadened by H_2 at 440 and 580 K, enlarging the range of temperatures of previous experiments.[4] As in Ref. 4 the experimental technique used is stimulated Raman loss spectroscopy.[6]

Furthermore, in order to compare with experimental results, we have built up a new *ab initio* potential energy surface (PES), using quantum chemistry methods, on which quantum calculations of the pressure broadening cross sections for N_2-H_2 have been performed.

In the following section we briefly describe the experimental device used in this study. In Sec. III we present the method employed for the *ab initio* calculations and the fitting procedure of the N_2-H_2 PES. Section IV is devoted to the pure quantum close coupling calculations. Results and discussions are included in Sec. V, and finally, concluding remarks and perspectives are given in Sec. VI.

II. EXPERIMENT

Experimental details have already been described in previous papers[4,6] and, therefore, only the high temperature Raman cell used for the measurements at 440 and 580 K will be given here. Figure 1 shows a scheme of the cell: a 60 cm long, 4 cm external diameter, and 1.7 cm internal diameter 316L stainless steel cylinder C1 constitutes the main body of the cell. 1 in. diameter fused silica windows W are fitted at both ends using isolast 8325 o-rings for 440 K and Loctite 5398 glue for 580 K. A perpendicular tube at the center of the cell houses a jacket for a thermocouple T1 and a pipe P for gas transfer. At 20 cm from the center another tube houses a second jacket for a second thermocouple T2 in order to control the temperature gradients. The main cell body is packed into four 68 Ω resistor muffles *M*. The total length of the four muffle assembly is 82 cm, exceeding the length

[a]Fax: +33 3 81 66 64 75. Electronic mail: pierre.joubert@univ-fcomte.fr

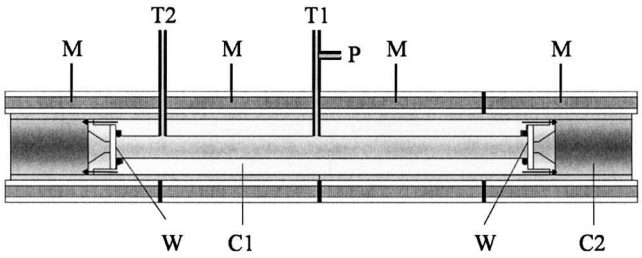

FIG. 1. Scheme of the high temperature Raman cell used for the measurements at 440 and 580 K.

of the main cell body by 22 cm in order to reduce as much as possible the temperature gradients between the window regions and the central part of the cell. A third 316L stain steel cylinder C2 is placed between the main body and the muffles, in close contact with both, in order to distribute as well as possible the heat flow in the border regions between muffles. The whole assembly is packed into a block of bored refractory bricks to provide thermal insulation.

The heating procedure is as follows: The desired temperature is set in a temperature controller built for this purpose. The controller compares the reading of the thermocouples with the target temperature, and a microprocessor determines the initial heating time of the four resistors, which are, at this stage, connected in parallel. The heating profile used by the microprocessor has been previously determined through measurements performed using the same cell in order to estimate the thermal inertia of the system. After this initial heating stage the reading of thermocouples should be approaching the desired value, and the system enters a second stage in which the heating is stopped (resistor voltage set to zero) while the temperature in the cell main body continues to slowly rise due to the inertia of the muffles.

Once the operation regime has been reached (typically in 60 min for about 500 K), the maximum temperature fluctuation over 3 h operation is estimated to be less than 1 °C. The gradient between thermocouples during this period is also estimated to be less than 1 °C.

III. A NEW N_2-H_2 INTERMOLECULAR POTENTIAL

Motivated by the scarce and no global previous works[7–9] on the ground state potential energy surface of N_2-H_2, we present here new *ab initio* calculations for this state in order to determine the potential energy of this dimer in a large range of geometries.

A. *Ab initio* calculations

First, we have used two different *ab initio* methods and several basis sets to test their influence on the binding energies. Indeed, as we are dealing with a van der Waals interaction, the binding energies are small and the precision on the energy must be higher than one wave number. For that, we have carefully chosen size-consistent methods: the symmetry-adapted perturbation theory[10] (SAPT) and the state of the art coupled cluster method including single and double excitations with perturbative treatment of triple excitations [CCSD(T)]. Three basis sets have been tested: augmented correlation consistent polarized triple zeta or quadruple zeta valence (aug-cc-pVTZ/aug-cc-pVQZ) basis sets and the polarization optimized one of Sadlej. All of them have been completed with a $(3s3p2d1f)$ set of midbond functions as proposed by Tao and Pan.[11] The aug-cc-pVTZ basis consists of $[5s4p3d2f]$ contracted Gaussian functions for N and $[4s3p2d]$ for H, the aug-cc-pVQZ set is contracted to $[6s5p4d3f2g]$ for N and $[5s4p3d2f]$ for H, and the Sadlej basis set has $[5s3p2d1f]$ contracted Gaussian functions for N and $[3s2p]$ for H. In order to obtain accurate intermolecular energies with the CCSD(T) method, we have to correct the CCSD(T) energies from the basis set superposition errors (BSSEs), while the SAPT method gives BSSE-free energies. The BSSE correction has been realized following the Boys and Bernardi approach.[12] For that, three calculations are required at each geometry: (1) $E_{AB}(AB)$, the energy of the dimer in the AB dimer basis; (2) $E_{AB}(A)$, the energy of the monomer A in the dimer basis; and (3) $E_{AB}(B)$, similarly for the monomer B. The BSSE-free dimer energies are then obtained by

$$V^{CCSD(T)} = E_{AB}(AB) - E_{AB}(A) - E_{AB}(B). \quad (1)$$

TABLE I. *Ab initio* characteristics of the N_2-H_2 intermolecular potential for selected conformations of the dimer using different *ab initio* methods and several basis sets: (a) CCSD(T) with aug-cc-pVTZ basis sets, (b) CCSD(T) with aug-cc-pVQZ basis sets, (c) CCSD(T) with Sadlej basis sets augmented with mid bond functions (MBFs), (d) SAPT with Sadlej basis sets+MBF, and (e) SAPT with aug-cc-pVTZ basis sets. Δ_1=c-d and Δ_2=d-e.

				Potential energy (cm^{-1})					
$\theta_A^{N_2}$ (deg)	$\theta_B^{H_2}$ (deg)	φ (deg)	R (Å)	(a)	(b)	(c)	(d)	(e)	Δ_1/Δ_2
0	0	0	4.02	−73.12	−73.46	−73.78	−69.74		−4.0
			4.23				−63.06	−65.45	+2.4
90	90	0	3.49	−58.47	−58.92	−58.48	−61.51		+3.0
			3.70				−54.58	−51.19	−3.4
90	90	90	3.49	−48.29	−48.76	−49.13	−51.16		+2.0
90	0	0	3.70	−31.77	−32.12	−32.59	−34.77	−30.00	+2.2/−4.8
0	90	0	4.23	−19.49	−19.43	−19.48	−19.00		−0.5
45	45	0	3.92	−27.12	−27.38	−28.39	−27.41		−1.0
22.5	67.5	0	4.13	−21.80		−22.31	−21.27		−1.0

We compare in Table I the potential energies obtained with the different methods and basis sets for selected dimer conformations. The conformations are characterized by four internal coordinates $(R,\theta_A,\theta_B,\varphi)$, where R is the intermolecular distance between the center of masses of both molecules, thus **R** is the oriented collisional axis (from N_2 to H_2). θ_A and θ_B define the orientations of the N_2 and H_2 molecules, respectively, relative to this axis, and finally φ defines the relative rotation about this axis. The diatomics have been treated as rigid and fixed at their vibrationally ground state distance, $r_0=2.074$ bohr for N_2 and $r_0=1.449$ bohr for H_2.

From columns (a), (b), and (c) of Table I, we note that the CCSD(T) method gives similar energies with the three selected basis sets that agree to better than 1 cm^{-1}, though the Sadlej basis is much smaller in size. Equivalent quantities obtained with the SAPT method as given by the Δ_2 values show stronger differences (up to ~ 5 cm^{-1}). The differences between the CCSD(T) and the SAPT values using the Sadlej basis are given by the Δ_1 quantity. We note that the use of a larger basis set (as given by Δ_2) partly compensates Δ_1 (as Δ_2 and Δ_1 have opposite signs). Nevertheless, only a few calculations have been conducted with the SAPT method and the aug-cc-pVTZ basis due to the difficulty of SAPT to converge with large basis sets, while the computational time grows up to several hours per point. Following these preliminary tests which give an accuracy of 4–5 cm^{-1} in the worst cases, we have selected the CCSD(T) method and the Sadlej basis set augmented with midbond functions to generate a regular grid of *ab initio* points in order to get the global PES. The CCSD(T) calculations have been done with the MOLPRO package.[13] 1575 *ab initio* points have been evaluated on a $(R,\theta_A,\theta_B,\varphi)$ grid of $R=[5.0,6.0,7.0,8.0,9.0,14.0,20.0]$ (in bohr), $\theta_A=\theta_B=[0.0°,22.5°,45.0°,67.5°,90.0°]$, and $\varphi=[0.0°,22.5°,45.0°,67.5°,90.0°,112.5°,135.0°,157.5°,180.0°]$.

B. Analytical fit of the potential energy surface

In order to analytically reproduce the above calculated points, we decomposed the intermolecular energies as follows:

$$E(R,\theta_A,\theta_B,\varphi)=E_{sh}(R,\theta_A,\theta_B,\varphi)+E_{as}(R,\theta_A,\theta_B,\varphi), \quad (2)$$

where E_{sh} and E_{as} represent, respectively, the short range contribution and the asymptotic long range part of the potential energy.

The short range contribution is given by

$$E_{sh}(R,\theta_A,\theta_B,\varphi)=G(R,\theta_A,\theta_B,\varphi)e^{D(\theta_A,\theta_B,\varphi)-B(\theta_A,\theta_B,\varphi)R}, \quad (3)$$

where G is a polynomial in R with the coefficients depending on the angles, and the exponential terms are assumed in the form

$$D(\theta_A,\theta_B,\varphi)=\sum_{L_A,L_B,L} d^{L_A,L_B,L}A_{L_AL_BL}(\theta_A,\theta_B,\varphi), \quad (4)$$

$$B(\theta_A,\theta_B,\varphi)=\sum_{L_A,L_B,L} b^{L_A,L_B,L}A_{L_AL_BL}(\theta_A,\theta_B,\varphi). \quad (5)$$

The angular functions $A_{L_AL_BL}(\theta_A\theta_B,\varphi)$ are defined in the case of two linear molecules by normalized product of spherical harmonics for monomers A and B as

$$A_{L_AL_BL}(\theta_A,\theta_B,\varphi)=\left(\frac{2L+1}{4\pi}\right)^{1/2}\sum_m \langle L_A m L_B -m|L0\rangle \times Y^m_{L_A}(\theta_A,0)Y^{-m}_{L_B}(\theta_B,\varphi), \quad (6)$$

where $Y^m_{L_A}$ and $Y^{-m}_{L_B}$ are ordinary spherical harmonics, $\langle\cdots|\cdots\rangle$ is a Clebsch-Gordan coefficient, and $|m|\leq\min(L_A,L_B)$.

The long range part of the potential is accounted for by the term

$$E_{as}(R,\theta_A,\theta_B,\varphi)=\sum_{L_A,L_B,L,n} f_n(B(\theta_A,\theta_B,\varphi)R)\frac{C_n^{L_AL_BL}}{R^n}A_{L_AL_BL}(\theta_A,\theta_B,\varphi), \quad (7)$$

where $f_n(B(\theta_A,\theta_B,\varphi)R)$ are damping functions given by Tang and Toennies.[14] The van der Waals constants $C_n^{L_A,L_B,L}$ are sums of the electrostatic, induction, and dispersion contributions obtained from the properties (multipole moments and static and dynamic polarizabilities) of the isolated monomers. The monomer multipole moments (Q_{L_A},Q_{L_B}) and dynamic polarizabilities have been evaluated up to the MBPT2 level. Then, the dispersion and induction coefficients are generated from the reducible frequency-dependent polarizabilities of each monomer followed by an integration over the imaginary frequency. All the asymptotic calculations and fitting procedure have been realized following the Bukowski *et al.* approach[15] as proposed in the related computer code.[16] $b^{L_A,L_B,L}$ and $d^{L_A,L_B,L}$ are coefficients obtained from the fit. The potential and the coefficients are available as a supplementary electronic support (EPAPS Ref. 28).

After a minimization of the root mean square (rms) quantity between the fitted and the *ab initio* energies, based on a nonlinear least square algorithm, we have obtained a rms of 0.01 kcal/mol for the global fit.

IV. CALCULATIONS OF PRESSURE BROADENING CROSS SECTIONS

Pressure broadening cross sections have been derived[17,18] from binary scattering *S*-matrix elements provided by MOLSCAT (Ref. 19) quantum dynamical code. Therefore, the impact approximation is assumed.[17,20,21] The coupled equations were solved by means of the hybrid log derivative-Airy propagator of Alexander and Manolopoulos.[22] The propagation is carried out with the diabatic modified log-derivative method from a minimum distance of 2 Å to an intermediate one of 15 Å and with the Airy method up to a maximum intermolecular distance $R=20$ Å. Convergence in the cross sections is typically reached for total angular momentum J varying approximately from 35 to 60 for kinetic energies between 68 and 513 cm^{-1}. Here $\vec{J}=\vec{j}_{AB}+\vec{l}$, in which $\vec{j}_{AB}$ is the composed an-

gular momentum formed by the two molecules and $\vec{l}$ is associated with the relative motion of the colliding pair. In order to economize CPU time, the analytical form of the present *ab initio* PES is not directly implemented in MOLSCAT but projected over 15 bispherical harmonics,[23]

$$V(R,\theta_A,\theta_B,\varphi)=\sum_{L_A,L_B,L} v_{L_A,L_B,L}(R)\times A_{L_AL_BL}(\theta_A,\theta_B,\varphi), \tag{8}$$

in which L_A, L_B, and L are even because the colliding pair is formed of homonuclear molecules and $|L_A-L_B|\leqslant L\leqslant|L_A+L_B|$. Note that this implies $\Delta j_A=\Delta j_B=0,\pm 2,\ldots$. The radial coefficients $v_{L_A,L_B,L}(R)$ were obtained through Gauss-Legendre quadratures over θ_A and θ_B and by a Chebyshev quadrature over φ.[24]

All energetically open rotational levels (j_A,j_B) and at least four asymptotically closed levels, defined by $E(j_A,j_B)=B_Aj_A(j_A+1)+B_Bj_B(j_B+1)$ in the rigid rotor approximations with $B_A=1.998$ cm^{-1} (for N_2) and $B_B=60.000$ cm^{-1} (for H_2), were included in the rotational basis to perform the scattering calculations for each total energy. Both nitrogen molecules and hydrogen molecules are composed of two noninterconverting species in our experiment. Natural nN_2 is a 2:1 mixture of ortho-(j_A even) and para-(j_A odd) species, while natural nH_2 is a 3:1 mixture of oH_2 and pH_2 species with odd and even j_B, respectively.

Finally, since we study isotropic Raman lines in the rigid rotor approximation, the reader should recall that pressure broadening cross sections are nothing but a sum of two-body rotational state to state cross sections $\sigma(j_A,j_B;E_{kin})=\Sigma_{j'_A,j'_B}\sigma(j_Aj_B\rightarrow j'_Aj'_B)$.

Pressure broadening cross sections were calculated over a grid of kinetic energies 5, 15, 30, 50, 55, 60, 65, 68, 75, 80, 85, 90, 120, 160, 210, 263.5, 389, and 513 cm^{-1}. The close coupling (CC) method is used for kinetic energy up to 389 cm^{-1}. In fact, the computational time remains reasonable up to this energy. The coupled states (CS) method is used to economize CPU time only for the highest energy considered, namely, 513 cm^{-1}. We have tested this approximation calculating the collisional cross section for the $Q(10)$ line at 440 K (corresponding to 389 cm^{-1}). We obtain 21.5 Å^2 using the CC method and 21.2 Å^2 using CS method. Therefore we assume that approximations introduced in CS calculations are quite reasonable at least for this temperature and above. Finally, note that $E_{kin}=68$, 263.5, 389, and 513 cm^{-1} are the kinetic energies associated with the mean relative speed $\bar{v}=\sqrt{8k_BT/\pi\mu}$ for the temperatures $T=77$, 298, 440, and 580 K, respectively, where $\mu=1.87$ amu is the reduced mass of the colliding pair.

To compare our calculations with the experimental pressure broadening coefficients we have taken into account both forms of H_2. Fortunately, the calculations can be greatly speeded up by dealing with the two forms separately, since for a given $Q(j_A)$ line

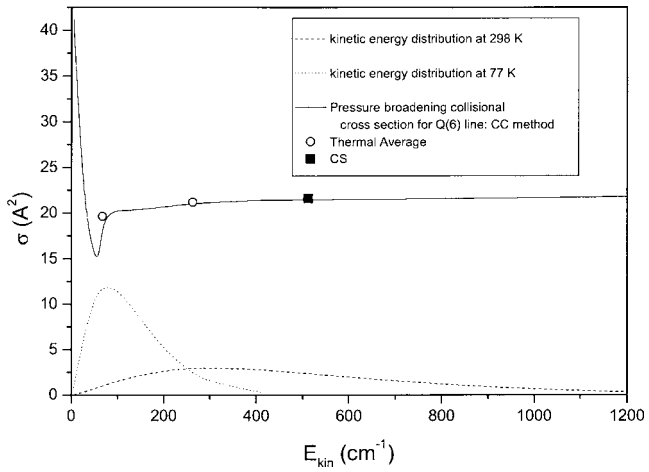

FIG. 2. Kinetic energy distribution of the perturber molecules of the system N_2-H_2 at 77 and 298 K (dotted and dashed lines, respectively), and pressure broadening collisional cross section for the N_2 $Q(6)$ line (solid line). The pressure broadening collisional cross section values (square) obtained by CS methods for 580 K (513 cm^{-1}) are also reported. The thermal averaged values (circle) of this parameter at 77 K (68 cm^{-1}) and 298 K (263.5 cm^{-1}) obtained by CC method are also included for comparison.

$$\gamma(j_A)=\frac{n_{H_2}\bar{v}}{2\pi c}\left\{\frac{3}{4}\sum_{j_B\text{odd}}\rho_{j_B}\bar{\sigma}(j_A,j_B)+\frac{1}{4}\sum_{j_B\text{even}}\rho_{j_B}\bar{\sigma}(j_A,j_B)\right\}. \tag{9}$$

Note that the thermal average $\bar{\sigma}$ of the cross sections over the energy distribution is performed independent of the H_2 unit normalized rotational populations ρ_{J_B}. We have compared our calculations with the pressure broadening coefficients measured at $T=77$, 298, 440, and 580 K. In the former case only the $j_B=0$ and 1 rotational states were included in the rotational basis (in separated MOLSCAT runs), because the population of other H_2 rotational levels is negligible, while at higher temperatures the first two rotational levels (for each H_2 species) were included in the rotational basis.

To save CPU time we did not perform the thermal average at 298, 440, and 580 K because the number of energetically accessible channels dramatically increases with the kinetic energy. This is a good approximation, as we have been able to test calculating the line broadening parameter of the $Q(6)$ line at $T=298$ K using thermal average. In this aim, calculations have been performed for higher kinetic energies (410, 430, 450, 600, 800, 1000, and 1200 cm^{-1}) and compared to the value that we have obtained using the cross section calculated at the corresponding mean relative kinetic energy. It must be noted that we have calculated thermal average for a single line in order to test this approximation because of the high computational cost using CC method at these temperatures. For $Q(6)$ line, the calculated broadening coefficients are 50.83×10^{-3} cm^{-1}/atm for the thermal average and 50.56×10^{-3} cm^{-1}/atm in the other case. This provides a difference of only 0.53% between both values (Fig. 2). Therefore we expect this approximation to be valid for all the lines.

In order to compare the CC and CS values with the measured ones we replaced $\bar{\sigma}$ by the cross sections calculated at $E_{kin}=263.5$, 389.0, and 513.0 cm^{-1}. This approxima-

TABLE II. Comparison between experimental and theoretical [close coupling (CC) or coupled states (CS)] values of the *Q*-branch line broadening coefficients [half-width at half maximum (HWHM)] of the N_2-H_2 system for several *j* and temperatures. All values are in mk atm^{-1} (1 mk$=10^{-3}$ cm^{-1}).

j	Expt. 77 K	CC 77 K	Expt. 298 K	CC 298 K	Expt. 440 K	CC 440 K	Expt. 580 K	CS 580 K
0	127.48(28.5)	121.90	58.2(12.0)	64.08	45.5(16.4)	53.49	44.9(39.3)	47.66
1	82.64(16.2)	74.17	49.5(9.8)	45.85	36.0(11.4)	···	50.3(17.6)	···
2	82.93(15.4)	85.2	45.4(4.3)	46.51	36.4(9.0)	39.60	47.1(15.0)	35.91
3	78.11(19.5)	89.24	50.6(6.9)	48.29	41.6(10.9)	···	36.5(17.2)	···
4	84.75(10.8)	92.39	46.5(3.8)	49.45	39.0(11.3)	41.48	25.5(10.3)	36.69
5	92.69(12.1)	91.90	44.6(5.6)	50.13	38.4(9.0)	···	32.1(11.8)	···
6	101.82(16.1)	92.62	47.8(4.6)	50.56	37.1(8.3)	42.31	31.2(11.2)	37.21
7	···	92.62	51.1(5.4)	50.85	40.1(6.5)	···	36.5(11.4)	···
8	···	92.77	46.4(3.4)	50.97	42.5(9.0)	42.58	40.2(10.3)	37.38
9	···	···	50.5(4.0)	50.92	38.9(8.1)	···	37.4(8.3)	···
10	···	···	48.6(4.0)	50.79	37.3(9.6)	42.62	35.9(11.8)	37.45
11	···	···	41.5(11.2)	50.47	42.6(6.2)	···	43.3(10.5)	···
12	···	···	···	···	43.1(5.3)	···	38.6(12.6)	37.44
13	···	···	···	···	40.7(9.5)	···	34.7(14.0)	···
14	···	···	···	48.87	38.6(6.7)	41.54	40.1(9.0)	37.28
15	···	···	···	···	42.9(9.3)	···	32.2(11.1)	···
16	···	···	···	···	33.4(6.1)	···	39.7(10.6)	36.98
17	···	···	···	···	32.3(19.6)	···	30.9(13.4)	···
18	···	···	···	···	34.2(6.0)	40.27	26.7(13.3)	36.48
19	···	···	···	···	···	···	22.6(17.7)	···
20	···	···	···	···	···	···	26.4(16.1)	35.83
21	···	···	···	···	···	···	39.9(9.3)	···
22	···	···	···	···	···	···	20.1(15.5)	35.01

tion can be expected to be quite accurate as the pressure broadening cross sections are slowly varying functions with increasing kinetic energy[4,25,26] [Fig. 2 for the $Q(6)$ line].

V. RESULTS AND DISCUSSION

A. Experimental measurements

We have measured new experimental *Q*-branch line broadening coefficients of nitrogen perturbed by hydrogen for several values of rotational quantum numbers *j* at temperatures of 440 and 580 K. The technique used was stimulated Raman loss spectroscopy. To this purpose, we designed and constructed a heating cell with a system of thermal stabilization, also developed in our laboratory, allowing us to extend considerably the range of temperatures previously studied.[4] In Table II, the old experimental results (77 and 298 K) and the new ones (440 and 580 K) are summarized.

B. *Ab initio* PES calculation

We have calculated a new potential energy surface for the N_2-H_2 system by testing different *ab initio* methods and basis sets in order to know the influence of both factors on binding energies. We have chosen to build the PES with the CCSD(T) method and the Sadlej basis set augmented with midbond functions. In Fig. 3 we present potential energy curves for some selected geometries of the dimer, in particular, for the most bound linear (*L*) one. From the fit, we get for this conformation a binding energy $D_c=-75.2$ cm^{-1} for an equilibrium distance $R_e=4.05$ Å. Binding energies and equilibrium distances for other conformations are presented in Table III and compared with the previous results of Salazar *et al.*[7] These authors have done fourth order many-body perturbation theory (MBPT4) calculations with two different basis sets, one with the medium sized POL1 basis set of Sadlej and one with POL1 augmented with a set of midbond functions (MBFs) [$3s3p2d$] of Tao *et al.*[11] We get a very good quantitative agreement with the values of Salazar *et al.*[7] when the energies are evaluated with the set of bond functions. The largest discrepancy (8 cm^{-1}) is observed for the linear absolute minimum. The agreement is only relatively good with the energies evaluated without the set of bond functions as they are always less bound and generate discrepancies up to 16 cm^{-1}.

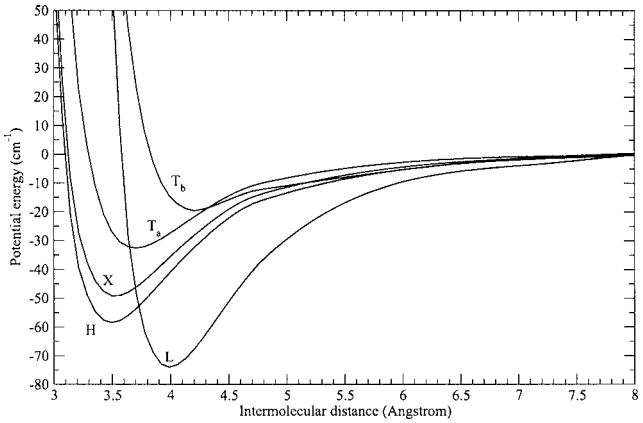

FIG. 3. Potential energy of N_2-H_2 as a function of the intermolecular distance *R* for some selected conformations of the dimer: $(\theta_A^{N_2}, \theta_B^{H_2}, \varphi) = (90°, 90°, 0°)$ for H, (0°, 0°, 0°) for L, (90°, 90°, 90°) for X, (90°, 0°, 0°) for T_a, and (0°, 90°, 0°) for T_b.

TABLE III. Binding energies and equilibrium distances of the N_2-H_2 potential obtained with the CCSD(T) method using the Sadlej basis sets augmented with midbond functions and comparison with the previous findings of Salazar *et al.* (Ref. 7).

$\theta_A^{N_2}$ (deg)	$\theta_B^{H_2}$ (deg)	φ (deg)		Present work	POL1 basis[a]	POL1+MBF[a]
0	0	0	R_e(Å)	4.05	4.02	
			D_e(cm^{-1})	−75.2	−67.35	−81.14
90	90	0	R_e(Å)	3.46	3.60	
			D_e(cm^{-1})	−58.78	−42.42	−59.77
90	90	90	R_e(Å)	3.75		
			D_e(cm^{-1})	−49.13		
90	0	0	R_e(Å)	3.75	3.86	
			D_e(cm^{-1})	−32.66	−23.39	
0	90	0	R_e(Å)	4.23	4.34	
			D_e(cm^{-1})	−19.48	−15.97	
45	45	0	R_e(Å)	3.92	4.07	
			D_e(cm^{-1})	−28.39	−20.49	−28.96
22.5	67.5	0	R_e(Å)	4.13		
			D_e(cm^{-1})	−22.31		

[a]Reference 7.

Present results confirm previous findings of Salazar *et al.*[7] Our findings are that the linear conformation is the most stable one, followed by the planar and parallel (H) configuration, then followed by the crossed (X) conformation, and finally, by the T shaped structures, which are the less bounded with binding energies of 33 and 19 cm^{-1} for H_2 pointing toward N_2 and conversely, i.e., (L>H>X>T).

C. Quantum line broadening calculations

Using the PES described above, we have computed pressure broadening coefficients of N_2 Raman isotropic Q branch at the temperatures of 77, 298, 440, and 580 K. In Table II and in Fig. 4, we present a summary of experimental and quantum line broadening coefficients for all the considered temperatures. It must be noted that the experimental values of the line broadening coefficient with the lowest and highest j values present larger error bars. It is due to the fact that these lines are the less intense ones of the spectrum for each studied temperature, and therefore they present the worst signal to noise ratio. In these cases, comparison between experience and theory is less significant than for the other lines considered. The relative average differences between experiment and calculations are 7.2% for 77 and 298 K, 10.7% for 440 K, and 22.3% for 580 K. If we do not consider the values corresponding to the first and last j for each temperature the differences are 7.4% for 77 K, 5.5% for 298 K, 10.1% for 440 K, and 18.7% for 580 K. The theoretical results are in very good agreement with experimental ones, taking into account the error bars of the experimental values, though as it can be seen, the agreement is better at lower temperatures. Theoretical calculations provide an interesting test of the potential energy surface presented in this work. The magnitude and temperature dependence are well reproduced for all j numbers in the whole range of temperatures. Further checks of the quality of this PES on the comparison between calculated and experimental second virial coefficients and scattering cross sections will be published in a forthcoming paper.[27]

VI. CONCLUSION

We have presented a detailed study of pressure broadening coefficients of nitrogen Raman Q-branch lines perturbed by H_2. For that purpose, new experimental and theoretical results concerning the N_2-H_2 system have been obtained. Line broadening coefficients are measured by the precise stimulated Raman loss spectroscopy technique and compared to calculations performed using quantum calculations on a new *ab initio* potential energy surface.

As it was discussed in a previous work,[4] the theoretical collisional line broadening coefficients, obtained from the semiclassical Robert-Bonamy model using an analytical atom-atom potential for the N_2-H_2 system at 77 and 298 K, show a discrepancy with respect to the experimental values, mainly for 77 K. For low temperatures, semiclassical approaches are not well adapted for line broadening calculations due to contribution of orbiting collisions not taken into account in the model. In this case, only pure quantum methods (as CC or CS) can be used. Indeed, comparison between experimental data (77–580 K) and the theoretical results carried out in this work shows that the new potential energy surface presented in this paper allows us to reproduce quite well the broadening coefficients and their temperature dependence.

Temperature diagnostic in combustion media requires high temperature broadening coefficients, but due to the computational cost for pure quantum calculations (CC or CS methods) at high temperatures, only semiclassical approaches[5] are feasible. Following the previous work[4] done with the Robert-Bonamy approach, new calculations must be performed to determine the temperature dependence of line

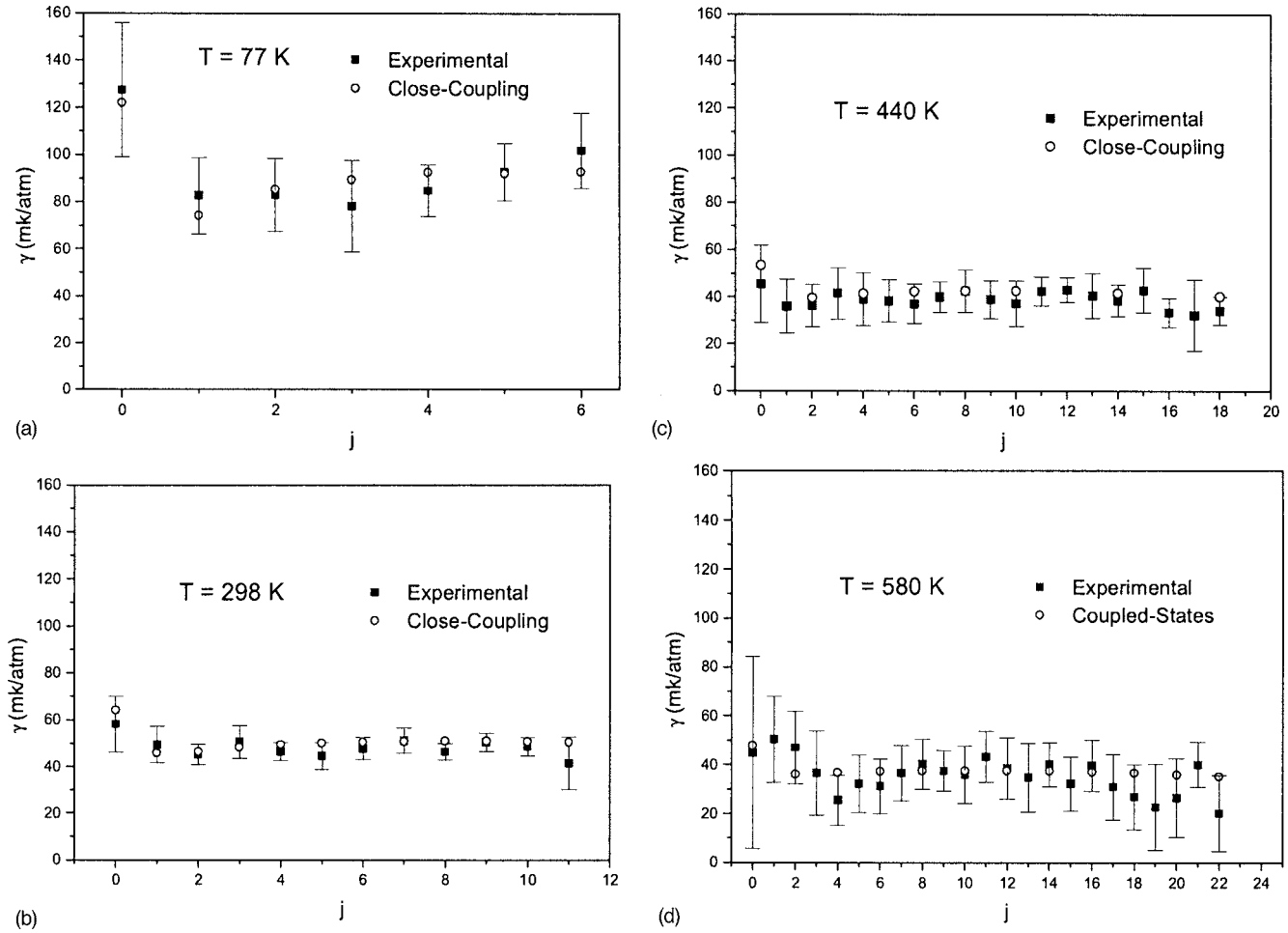

FIG. 4. Comparison between experimental and theoretical values of the *Q*-branch line broadening coefficient (HWHM) for several *j*, in mk atm^{-1}, (a) for $T=77$ K, (b) for $T=298$ K, (c) for $T=440$ K, and (d) for $T=580$ K.

broadening coefficients at high temperatures (up to 2500 K). Due to the satisfactory results obtained with the present *ab initio* PES, these calculations require the implementation of this potential in the RB model. This work is in progress and will be presented in a future paper.

ACKNOWLEDGMENTS

The authors would like to thank the Institut du Développement et des Ressources en Informatique Scientifique (IDRIS, CNRS) for providing the authors with the computer power as well as the "Pôle de Calcul Informatique de l'Ouest (PCIO)" located in Rennes. Three of the authors (L. G., R. M., and D. B.) would like to thank Robert Saint-Loup for kindly providing technical information for the construction of the high temperature cell, and Javier Rodriguez for design and construction of the electronic stabilization. Finally the said authors (L. G., R. M., and D. B.) also acknowledge financial support from Spanish DGI under Project No. FIS2005-02029.

[1] B. Lavorel, G. Millot, R. Saint-Loup, C. Wegner, H. Berger, J. P. Sala, J. Bonamy, and D. Robert, J. Phys. (Paris) **47**, 417 (1986).
[2] L. A. Rahn and R. E. Palmer, J. Opt. Soc. Am. B **3**, 1164 (1986).
[3] J. Bonamy, L. Bonamy, D. Robert, M. L. Gonze, G. Millot, B. Lavorel, and H. Berger, J. Chem. Phys. **94**, 6584 (1991).
[4] L. Gomez, D. Bermejo, P. Joubert, and J. Bonamy, Mol. Phys. **104**, 1869 (2006).
[5] D. Robert and J. Bonamy, J. Phys. (Paris) **40**, 923 (1979).
[6] D. Bermejo, J. Santos, P. Cancio, J. L. Doménech, C. Domingo, J. M. Orza, J. Ortigoso, and R. Escribano, J. Raman Spectrosc. **21**, 197 (1990).
[7] M. C. Salazar, J. L. Paz, and A. J. Hernandez, J. Mol. Struct.: THEOCHEM **464**, 183 (1999).
[8] S. P. Walch, J. Chem. Phys. **91**, 389 (1989).
[9] J. R. Stallcop, H. Partridge, and E. Levin, Phys. Rev. A **62**, 062709 (2000).
[10] SAPT, a program for many-body symmetry-adapted perturbation theory calculations of intermolecular interaction energies, 1999; B. Jeziorski, R. Moszynski, A. Ratkiewicz, S. Rybak, K. Szalewicz, H. L. Williams, B. Jeziorski, R. Moszynski, and K. Szalewicz, Chem. Rev. (Washington, D.C.) **94**, 1887 (1994); R. Moszynski, P. E. S. Wormer, and A. van der Avoird, in *Computational Molecular Spectroscopy*, edited by P. R. Bunker and P. Jensen (Wiley, New York, 2000), p. 69.
[11] F. M. Tao and Y. K. Pan, Mol. Phys. **81**, 507 (1994); J. Chem. Phys. **100**, 4947 (1994).
[12] S. F. Boys and F. Bernardi, Mol. Phys. **19**, 553 (1970).
[13] H.-J. Werner, P. J. Knowles, R. D. Amos *et al.*, MOLPRO version 2002, a package of *ab initio* programs.
[14] K. T. Tang and J. P. Toennies, J. Chem. Phys. **80**, 3726 (1984).
[15] R. Bukowski, J. Sadlej, B. Jeziorski, P. Jankowski, K. Szalewicz, S. A. Kucharski, H. L. Williams, and B. M. Rice, J. Chem. Phys. **110**, 3785 (1999).
[16] R. Bukowski, J. Sadlej, B. Jeziorski, P. Jankowski, K. Szalewicz, S. A. Kucharski, H. L. Williams, and B. M. Rice, ASYMP-SAPT package, University of Delaware and University of Warsaw.

[17] A. Ben-Reuven, Phys. Rev. **141**, 34 (1966); **145**, 7 (1966).
[18] R. Shafer and R. G. Gordon, J. Chem. Phys. **58**, 5422 (1973).
[19] J. M. Hutson and S. Green, MOLSCAT version 14, Collaborative Computational Project 6 of the UK Science and Engineering Research Council, Daresbury Laboratory, UK, 1995.
[20] M. Baranger, Phys. Rev. **111**, 481 (1958); **112**, 855 (1958).
[21] U. Fano, Phys. Rev. **131**, 259 (1963).
[22] M. H. Alexander and D. E. Manolopoulos, J. Chem. Phys. **86**, 2044 (1987).
[23] S. Green, J. Chem. Phys. **62**, 2271 (1975).
[24] W. H. Press, B. P. Flannery, S. A. Teukolsky, and W. T. Vetterling, *Numerical Recipes in Fortran 77, The Art of Scientific Computing* (Cambridge University Press, Cambridge, 1992), Chap. 4.
[25] F. Thibault, B. Calil, J. Buldyreva, M. Chrysos, J. M. Hartmann, and J. P. Bouanich, Chem. Phys. **3**, 3924 (2001).
[26] F. Thibault, R. Z. Martinez, J. L. Domenech, D. Bermejo, and J. P. Bouanich, Chem. Phys. **117**, 2523 (2002).
[27] L. Gomez, T. Cauchy, M. Bartolomei, D. Cappelletti, F. Pirani, and B. Bussery-Honvault, Chem. Phys. Lett. (unpublished).
[28] See EPAPS Document No. E-JCPSA6-126-017718 for the potential routines including the coefficients. This document can be reached via a direct link in the online article's HTML reference section or via the EPAPS homepage (http://www.aip.org/pubservs/epaps.html).